Primary effusion lymphoma: genomic profiling revealed amplification of *SELPLG* and *CORO1C* encoding for proteins important for cell migration

Shi-Lu Luan,[1] Emmanuelle Boulanger,[2,3] Hongtao Ye,[1] Estelle Chanudet,[1] Nicola Johnson,[1] Rifat A Hamoudi,[1] Chris M Bacon,[4] Hongxiang Liu,[1] Yuanxue Huang,[1] Jonathan Said,[5] Peiguo Chu,[6] Christoph S Clemen,[7] Ethel Cesarman,[8] Amy Chadburn,[8] Peter G Isaacson[9] and Ming-Qing Du[1]*

[1] *Department of Pathology, University of Cambridge, Cambridge, CB2 0QQ, UK*
[2] *Department of Clinical Immunology, Hôpital Saint Louis, Paris, France*
[3] *Greehey Children's Cancer Research Institute, The University of Texas Health Science Center at San Antonio, San Antonio, Texas, USA*
[4] *Northern Institute for Cancer Research, Newcastle University, Newcastle upon Tyne, NE2 4HH, UK*
[5] *Department of Pathology and Laboratory Medicine, David Geffen School of Medicine, University of California-Los Angeles, Los Angeles, CA 90095, USA*
[6] *Division of Pathology, City of Hope National Medical Centre, Duarte, CA 91010, USA*
[7] *Center for Biochemistry, Institute of Biochemistry I, Medical Faculty, University of Cologne, Cologne, Germany*
[8] *Department of Pathology and Laboratory Medicine, Weill Medical College of Cornell University, New York, NY 10065, USA*
[9] *Department of Pathology, University College London, London, WC1E 6JJ, UK*

Correspondence to: Professor Ming-Qing Du, Division of Molecular Histopathology, Department of Pathology, University of Cambridge, Level 3 Lab Block, Box 231, Addenbrooke's Hospital, Hills Road, Cambridge, CB2 2QQ, UK. e-mail: mqd20@cam.ac.uk

Abstract

Primary effusion lymphoma (PEL) is associated with Kaposi sarcoma herpesvirus (KSHV) but its pathogenesis is poorly understood. Many KSHV-associated products can deregulate cellular pathways commonly targeted in cancer. However, KSHV infection alone is insufficient for malignant transformation. PEL also lacks the chromosomal translocations seen in other lymphoma subtypes. We investigated 28 PELs and ten PEL cell lines by 1 Mb resolution array comparative genomic hybridization (CGH) and found frequent gains of 1q21–41 (47%), 4q28.3–35 (29%), 7q (58%), 8q (63%), 11 (32%), 12 (61%), 17q (29%), 19p (34%), and 20q (34%), and losses of 4q (32%), 11q25 (29%), and 14q32 (63%). Recurrent focal amplification was seen at several regions on chromosomes 7, 8, and 12. High-resolution chromosome-specific tile-path array CGH confirmed these findings, and identified selectin-P ligand (*SELPLG*) and coronin-1C (*CORO1C*) as the targets of a cryptic amplification at 12q24.11. Interphase FISH and quantitative PCR showed *SELPLG/CORO1C* amplification (>4 extra copies) and low levels of copy number gain (1–4 extra copies) in 23% of PELs, respectively. Immunohistochemistry revealed strong expression of both SELPLG and coronin-1C in the majority of PELs, irrespective of their gene dosage. SELPLG is critical for cell migration and chemotaxis, while CORO1C regulates actin-dependent processes, thus important for cell motility. Their overexpression in PEL is expected to play an important role in its pathogenesis.
Copyright © 2010 Pathological Society of Great Britain and Ireland. Published by John Wiley & Sons, Ltd.

Keywords: primary effusion lymphoma; CGH; *SELPLG*; *CORO1C*; gene amplification

Introduction

Kaposi sarcoma herpesvirus (KSHV) is directly associated with Kaposi sarcoma and several lymphoproliferative disorders (LPDs) including primary effusion lymphoma (PEL)/extra-cavitary PEL (EC-PEL or solid PEL), multicentric Castleman disease (MCD) and germinotropic LPD [1,2]. Among these different LPDs, PEL is the most common and best characterized. PEL and EC-PEL are both very aggressive lymphomas [3] and are indistinguishable in their morphological and immunophenotypic features; they are thus considered to be different anatomical manifestations of the same

disease [1,4]. The tumour cells usually express CD45, lack expression of B-cell markers and immunoglobulin, but are commonly positive for CD138 and other plasma cell antigens and are co-infected by Epstein–Barr virus (EBV) [1]. Southern blot analyses of the rearranged immunoglobulin genes show that most PELs are monoclonal [5].

Over the last decade, there has been a steady advance in our understanding of the oncogenic activities of a number of KSHV-encoded products. In PEL, KSHV is at latency in the vast majority of tumour cells [6]. In general, it is believed that the viral products produced in latency are most directly

involved in malignant transformation [6]. Among the latently expressed genes, LANA-1, viral cyclin, viral FLICE inhibitory protein, and LANA-2 are consistently expressed in most KSHV-infected lymphoma cells [7–12]. These viral oncogenic proteins have been shown to deregulate a number of cellular pathways commonly targeted in human cancer and are capable of cooperating with cellular oncoproteins in malignant transformation [1,2]. Despite this, KSHV infection alone is clearly insufficient for malignant transformation as the incidence of KSHV-associated lymphoma in populations with high KSHV seroprevalence is remarkably low. In addition, EBV is unlikely to play a major role in PEL development since the lymphoma cells do not express the EBV-transforming antigens LMP2 and EBNA2 [13–15]. The acquisition of genetic abnormalities is therefore likely to play a critical role in the development of KSHV-associated lymphoma. Conventional cytogenetic analysis of a small number of cases of PEL showed complex karyotypes, with recurrent trisomies 7, 8, and 12 but no recurrent structural abnormalities [16–18]. Chromosomal translocations seen in other non-Hodgkin lymphomas, such as those involving the *CCND1, BCL2, BCL6*, and *MYC* loci, are consistently absent in PEL [5,19]. In the present study, we investigated the genomic profiles of 28 PELs and ten PEL cell lines using 1 Mb resolution array comparative genomic hybridization (CGH) and further characterized recurrent genomic amplifications by high-resolution tile-path array CGH, interphase FISH, quantitative PCR, immunohistochemistry, and western blot.

Materials and methods

Patients and cell lines

A total of 37 cases of PEL, including nine EC-PELs, and 14 PEL cell lines were investigated. The histological and immunophenotypic features of 17 PELs have been described previously [4,20]. The diagnosis of PEL was established according to the criteria of the recent WHO classification [21]. High-molecular-weight DNA samples from 28 primary cases including four EC-PELs, and ten PEL cell lines were used for CGH and quantitative PCR. All DNA samples used for array CGH and quantitative PCR contained at least 70% of tumour cells. Formalin-fixed, paraffin-embedded (FFPE) cell clots from ten PELs and nine PEL cell lines, and FFPE tissues from eight EC-PELs were used for FISH and immunohistochemistry. The use of archival tissues for research was approved by the ethics committees of the institutions involved.

DNA amplification and quality assessment

The quality of the DNA samples was assessed by PCR and only those with successful amplification greater than 300 bp were subjected to array CGH [22]. In four primary cases, the quantity of available DNA was insufficient and these DNA samples were amplified using the Genomeplex™ WGA kit (Rubicon Genomics, Ann Arbour, USA) prior to array CGH [22].

Array CGH

Genomic profiles were obtained using in-house 1 Mb resolution genomic arrays as described previously [22]. The primary data were analysed using Microsoft Excel and genomic changes involving two or more consecutive clones were identified by an integrated approach combining visual inspection, assessment by a hidden Markov model, and statistical analysis with the mean ± 3 SDs ($\log_2$ value ± 0.19) from normal male/female hybridization used as the threshold [22,23].

A high-resolution tile-path array (91–118 kb) containing 1515, 1358, 1417, and 720 analysable BAC/PAC clones in duplicate for chromosomes 7, 8, 12, and 14, respectively, was constructed. CGH using this tile-path array was similarly performed. All array CGH results are provided in the Supporting information.

Interphase FISH

BAC clones RP11-266G20 (SELPLG/CORO1C, 12q 24.11) and RP11-804C24 (IL21, 4q27) were labelled with Spectrum Orange by nick translation (Abbott Laboratories, Maidenhead, UK), validated on metaphase spreads. The labelled probes together with CEP12 or CEP4 (Abbott Laboratories), and an *MDM2/*CEN12 probe (ZytoVision, Bremerhaven, Germany) were used for interphase FISH on FFPE cell clots or tissue sections [23]. Each of the FISH probes was investigated in eight to ten reactive tonsils and the value of the mean ± 3 SDs was used as the threshold to diagnose copy number changes [24]. Gain of one to four extra copies was recorded as low-level copy number gain, while gain of more than four extra copies was considered as amplification.

Quantitative PCR (qPCR)

The *SELPLG* and *CORO1C* gene dosage was determined by qPCR, with the *MGAT2* gene (14q21.3) as a reference control, which showed no copy number changes by array CGH (Supporting information, Supplementary methods). qPCR for each of these genes was carried out in triplicates using iQ SYBR Green supermix (Bio-Rad, Hemel Hempstead, UK) on an iCycler iQ system (Bio-Rad) [25]. The ΔCT value was calculated by subtracting the CT value of target genes from that of *MGAT2*.

Immunohistochemistry and western blot

Antibodies to SELPLG, coronin-1C [26,27], MDM2, and CD123, a marker for plasmacytoid dendritic cells [28], and the protocols for immunohistochemistry and western blot are described in detail in the Supporting information, Supplementary methods. The immunostaining was scored according to the percentage of positivity (<30%, 30–70%, >70% cells) and the intensity
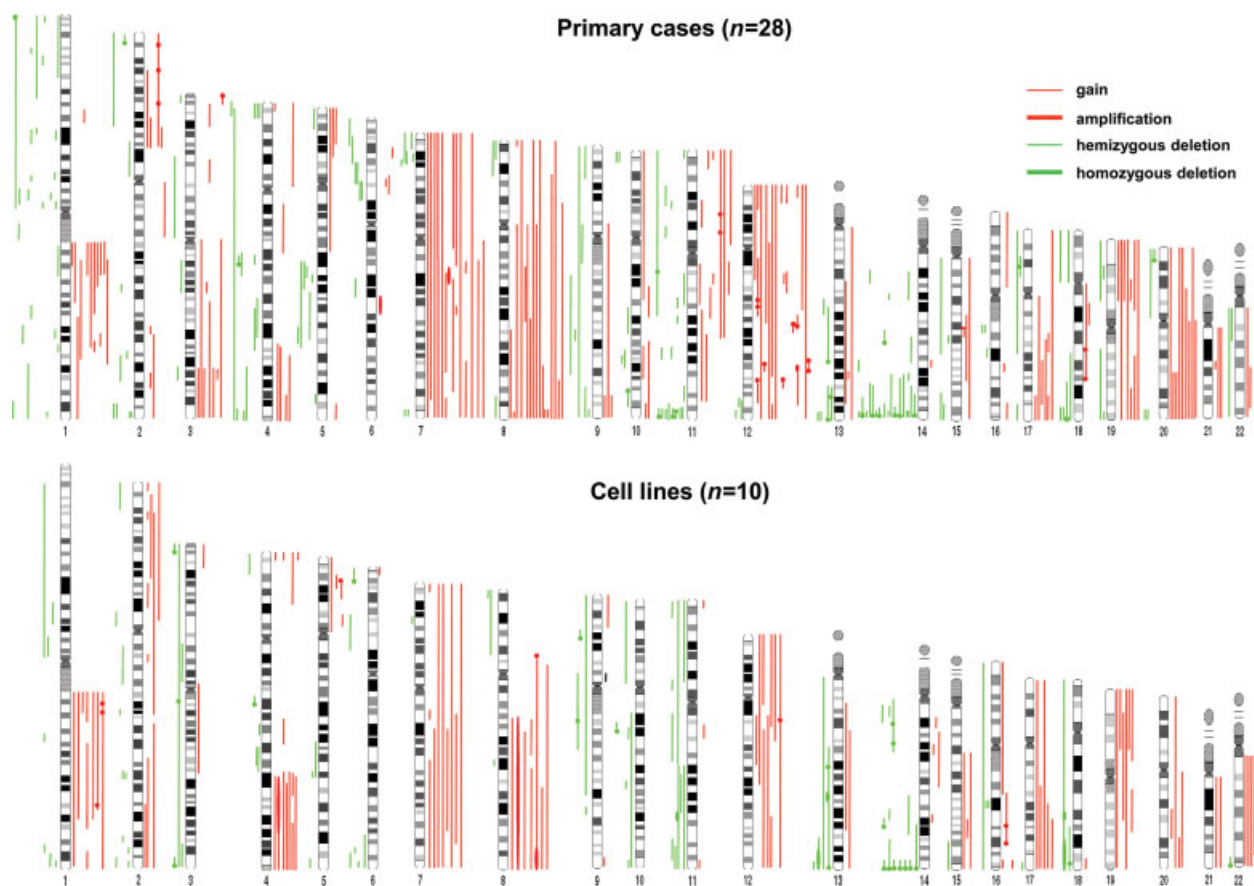
Figure 1. Genomic profiles of PEL by 1 Mb array CGH. Alterations that cannot be distinguished from normal copy number variation are indicated by a black line.

of immunostaining (weak, moderate, strong). Cases were considered positive if 30% or more of the tumour cells were stained.

Results

1 Mb genomic profile of primary PEL and PEL cell lines

1 Mb array CGH was successfully performed in 28 PELs including four EC-PEL, and ten PEL cell lines. With the exception that gain of 11q12–13 and 13q was more frequent in EC-PEL (3/4 and 2/4, respectively) than in PEL (3/23 and 1/23, respectively) ($p = 0.022$ and $p = 0.045$, respectively), there were no other apparent differences in the pattern and frequency of genomic imbalances between PEL and EC-PEL. Thus, the genomic profiles of PEL and EC-PEL were combined together (Figure 1). There was a strong similarity in the genomic imbalances between primary cases and cell lines, although gain of 4q was more frequent in cell lines than in primary cases (7/10 and 4/28, respectively; $p = 0.002$; Tables 1 and 2, Figure 1). Given this high degree of similarity, the major recurrent genomic imbalances in primary cases and cell lines were analysed together.

Overall, 26/28 primary cases and 10/10 cell lines showed extensive genomic imbalances (Supporting

information, Supplementary Figure 1). There were no matched normal DNA samples available to exclude the possibility of normal copy number variation (CNV). Nonetheless, CNV was rarely seen at the level of 1 Mb resolution using the threshold defined in this study and only one alteration at 9p11.2 in a cell line was potentially a CNV (http://cnv.chop.edu; http://projects.tcag.ca/variation) [29]. Although the genomic alterations involved every chromosome, there was no deletion of 17p13 (*TP53*) or 13q14 (*RB*). The most frequent genomic imbalances were gains of 1q21–41(18/38 = 47%), 4q28.3–35 (11/38 = 29%), 7q (22/38 = 58%), 8q (24/38 = 63%), 11 (12/38 = 32%), 12 (23/38 = 61%), 17q (11/38 = 29%), 19p (13/38 = 34%), and 20q (13/38 = 34%), and deletions of 4q (12/38 = 32%), 11q25 (11/38 = 29%), and 14q32 (24/38 = 63%). In the majority of cases, these recurrent genomic imbalances involved gain of one to three extra copies or deletion of only one copy of the respective chromosomal regions. Nonetheless, within these recurrent chromosomal gains or deletions, several loci showed amplification ($\geq$ four extra copies) or homozygous deletion, thus allowing mapping of the minimal common region (MCR) affected and the identification of potential target genes.

Of the five samples showing deletion at 4q26–28.2, RP11-364P2 was 'retained' in four cases, despite being within this deleted region (Figure 2). In addition, this

Table 1. Chromosomal gains and losses in PEL primary cases identified by 1 Mb array CGH analysis

Case No	Diagnosis	EBV infection	Chromosomal changes*	
			Gains	Losses
1	PEL	−	5p15–q14.2, 8q22.2–24.3, 12p13–q13.13	7p21.3, **14q32.2–32.33**, 22q11
2	PEL	+	1q21–25, 1q32, 2q32–37, 4p, 7q11.23, 7q32–36, 8p22–q24, 11p–q21, 12p13, **12q15–21.31, 12q23–24**, 19p, 19q13, 20, 22q13	**2p25**, 3q25, 4q22–23, 5q14.3–22, 6p24–22, 9q22, 10q24–25, 11q24–25, 13q34, 14q32.33, 15q26, **17p12**
3	PEL	+	1q21, 2p24.1–13, 3q26–29, 4q31–35, 8p23, 8q, 12p13, **12q12–15, 12q24** (.11–.31)	1p31.1, 1p21, 1p13–12, 1q31, 14q12–21.2, 14q31, 14q32.33, 16q21
4	PEL	+	1p31.3, 2p16.1–13, 2q32.2, 2q35–36, 7q21–32, 7q36, 10q24.2–25.3, 10p15–q22.2, 15q15–25.1, 16p11.2, **18q11.2–21.2**, 20q13, 21q	1p12–11, 1q24–25, 2q31.1, 3q13, 5q15, 6p22.1–21.31, 6q16, 7p21, 8p23, 8q24.2–.3, 9p24–22, 9q34, 10q22.3–23.2, **10q26**, 11q13.1–.2, 11q14.1, **11q25, 13q21–31, 13q32–34**, 14q23.2, 14q32, 16q12, 18q21.3–23
5	PEL	+	1q21–24, 8, 12, 17q, 20	14q32.33, 18q21–23
6	PEL	−	12	11q25, 13q34, 14q32.33
7	PEL	+	1q25.3–44, 3q26–29, 6q13, 8q13–21.3, 11p14.1–12, 11q13.5–24.2, **12q23.3**, 21q21.2	1p36–32.3, 5p15, 5q35, 6p21, 7p22, 12q24
8	PEL	+	4q31–35, 8q, 13q31	1p11, 2q37.3, 4p16, 4q26–28, 7p21.1, 12q24.31, 14q32
9	PEL	−	3q, 7, 8q21.3–24, 9p11–q34, 12p13–q15	1q44, 2q37.3, **14q31.3–32**, 15q21.2
10	PEL	−	8p23.2–q24, 11q21–24, 12p11–q24	1p36.3, 4q27–31.2, 6p22.1–21.31, 7q36.3, 9q34.3, 10q24.3, 11q25, **14q32.33**
11	PEL	−	7, 8q, 12p13–q24.11, 12q24.3	1p31.1, 14q32.33
12	PEL	+	1q21–23, 1q31–32, 6p22	2q24.2, 2q33–35, 4q22, 5q31, 6p25–23, 8p23–21, 9q21–32, 11p15.1–14.1, 11p11.2, 11q25, 12q24.33, **14q31.3–32.33**, 15q11–22, 15q26, 18q23, 20q13.3
13	PEL	−	1q21–32, 3q26–29, 4q13–22.1, 7p22–q36.1, 17q23–25.2, 19p13	1p35, 1p11, 4q22, 5q21, 11q25, 14q32
14	PEL	+	7q11.23–36, 8q24, 11p	1p13, 1q12, 4q35
15	PEL	+	4q34–35, 5p15–13.3, 7, 11p15	1p36.11, 1p31.1, 1p21, 5q21–31, **13q32–34**, 18p
16	PEL	+	**1q21–32**, 2p15–13, **3p26**, 3q, 4q31–35, 7q, 8p11–q24, **12q23**, 20q	**1p**, 1q43–44, 2p25–16, 2q37, 3p22–12, 4p16, 10p15, **11p15–q13, 11q25, 14q32.2–32.33**, 17p13–21, 17q25.3, 18p, 18q23, 19p13.2, 19q13.4, 20q13.3
17	PEL	−	7, 8, 12, 19, 20q13	4p16, 14q24.2–31.1, 14q32.33, **20p13**
18	PEL	−	**2p**, 6p21, 7, 8, 10q26.3, 12p13–q14, 17,19	2q37, 10p15, 11q22, 14q12–13.2, 14q32
19	PEL	−	1q21–31, 7p22–q11.21, 7q21–35, 19p13, 20	1q32–44, 4q35, 9, 13q14
20	PEL	+	12p13, **12q23–24.2**, 15q	2p13.1–11.2, 7p22–21.3, 7q36.3, 9p11–q12, **14q32.33**
21	PEL	+	3p25, 3p21, 3q21–29, 6p21.3, 7, 8q24.3, **11p15–q21, 12q21.2**, 18q12, 19p13.1, 19q13.2–13.4, 20q, 21q	3p26, 11p14.1, 11q22, **11q25**, 16q12, 20p
22	PEL	−	1q21–23, 7p–q11.2, 7q22.1, 8q24.3, 9q34, 10q22, 10q23–26, 11p15.5, 11q12–13.2, 12p13, 12q13, 16p13–11.2, 16q24, 17q21.3, 17q25, 19, 20p11–q, 22q	1q25.3–31, 4p15.3–q
23	PEL	−	None	None
24	PEL	+	None	None
25	Extra-cavitary PEL	+	13q14–33, **15q21.2**	1p36–34, 1q21–23, 1q32.1, 4p16, 6p21, 11p15.5, 11q12.3–13, 11q23.3–24, 14q23–24, 14q32, 19p13, 19q13, 22q
26	Extra-cavitary PEL	+	4p16, 8q24.3, 9q34, 11q12–13, 16q22, 17q25	None
27	Extra-cavitary PEL	+	1q21–23, 2q11.1–21, 3q13.31–13.33, 5p15–14, 5q35, **6q21, 7q11.23–21.1**, 11q13.2–14.1, 12q13.1, 13q, 14q24.3, 17q21.3–25, 20	4q32–35
28	Extra-cavitary PEL	+	1q21–22, 3q25, 11q12–13	None

*Chromosome regions in bold denote amplification or homozygous deletion.

Table 2. Chromosomal gains and losses in PEL cell lines identified by 1 Mb array CGH analysis

Cell line	EBV infection	Chromosomal changes*	
		Gains	Losses
BC1	+	1q21–41, 2q33–37, 7, 8q21–24, 9p24–22, 12p13–q21, 15q15–26	**14q32.33**
BC3	–	1q21, 7, 12q13–24, 19p13	1q43–44, 2q32.1, **4q22**, 6q27, **13q14–34**, 16q21
BC2	+	1q21–23.1, 1q24.1–42.13, 1q43–44, 2p25.1–15, 4q31–35, 6p25, 12p13–q13.2, 12q24, 14q12, 17q21.32–25, 19p13.2–q13.2, 20q13.2–13.3, 21q, 22q	1p, 1q23.3, 1q42.3, 2q12–14.3, 2q32.1, 2q36.2, **3**, 5q23.3, 6q25.3, 9p24–q31.1, 9q32, 10p, 10q23.3–24.1, **11**, 13q, 16
JCS1	+	1q21–43, 4p16, 4q28–35, 7p22.3, 7q11.23, 7q22–36, 8q13–24, 9q34, 14q31, 16p13.3–q13, 17, 18q23, 19, 20q13.1, 21q, 22q	1q44, 6q25–27, 10q21–26, 11p15–11.2, 11q14–25, **14q31.3–32.33**, 16q21
BCP1	–	1q21–41, 2p24.1–q22, 2q23.3–37, 3p26–25, 4p16–15, 4q28.3–31.22, 4q32–35, 7, **8p11–q24**, 15q22–24, 17q23–25, 19p13	2p25, 2q23.1, **6p25–24**, 8p23–12, **9p11–q21. 32**, **10q21.3**, 11q24–25, **14p11–21**, **14q32.33**, 15q25–26, **18**
BBG1	+	**1q21–44**, 2p25–11.2, 4p16, **5p15.2–14**, 5p13–12, 7, 8p11.2–q24, 11p15.5–15.4, 11q13, 13q14–34, 15q14–26, 16q24, 17q23–25, 19p13–11, 19q11–13.32, 20q, 22q	3p26, 3q29, 14q11–12, **14q31.2**, **14q32.33**
CRO-AP2	+	**1p23–32.2**, 4q28–35, 5p15.2–14.3, 7q11.23–35, 8q23–24.2, **12**, 22q11.2–13.2	1p13.2–11, 2p12–q11, 2q37, 4p16, 6p22–21, 6q25.3–27, 8p23, 11p15, 11p11.2, 11q12–13, 11q23.3–25, 13q34, 14q11.2, 14q24.3, **14q32, 22q13.3**
CRO-AP3	–	2p25.3, 2p24, 2p14–12, 2q13, 2q31–37, 3p11–22, 4p16, 4q23–25, 4q28–35, 8q13–21.13, 8q22–24, 12p13–q12, 12q13.2–24.31, 14q21.2, 20	1p22–21, 2q36, 2q37.3, 3p14–12, 3q27–29, 4q26–28.1, 5q21.3–23, 7p15, 8q21.3, 10q21, 10q26, 11q14.3–22.3, **14q32.33**, 17q25, **18q21–23**
CRO-AP5	+	4q28–35, 5p, 7q21–36, **8q13–24**, 11q25, 12q13–15	4q23–24, 4q26–28.1, 14q23.3–31, **14q32.32–32.33**
CRO-AP6	–	4q28–35, 7q21–34, 12p13–q13, 13q13–32.1, 14q13–23, **16q13–23**, 17, 19, 22q	5q35, **9q21.3**, **13q33–34**

*Chromosome regions in bold denote amplification or homozygous deletion.

BAC clone was gained notably in one case (Figure 2, case 3) and moderately in four further cases (Figure 2, case 18). A search of this region revealed *IL21* and *CCNA2* as potential targets of the gain.

Of the 22 samples showing gain of 7q, one showed approximately six copies at 7q11.23–21.11 spanning a region of 8.24 Mb. Potential target genes in the region showing the highest amplification included CD36 (thrombospondin receptor) and hepatocyte growth receptor (Supporting information, Supplementary Figure 2) [30]. Among the 24 cases showing gain of 8q, two showed a moderate amplification at 8q24, where the *MYC* gene is located (Supporting information, Supplementary Figure 3).

The most remarkable amplifications were those seen on chromosome 12, which involved three regions (Figure 3). The first amplification involved a region of 14.7 Mb at 12q13.2–15 and was seen in one primary case (No 3). A low level of gain of this region, often as part of the gain of chromosome 12 or 12q, was found in 11 additional cases. The second amplification involved a minimal common region of 170 kb at 12q21.2 and was seen in two primary cases (No 2 and 21). A low level of gain of this region as a part of the gain of chromosome 12 or 12q was seen in nine further cases. The third amplification involved a minimal common region of 3.28 Mb at 12q23.3–24.11 and was seen in five primary cases (No 2, 3, 7, 16, and 20).

Deletion at 14q32 was the most frequent loss (24/38 = 63%) in PEL, involving only the BAC clone RP11-417P24 in 12 cases. Hemizygous deletion of a 2.8 Mb region centromeric to the IGH locus at 14q32.31 was seen in 11/38 cases and interestingly, this region contained a cluster of 39 microRNAs (Supporting information, Supplementary Figure 4).

Characterization of chromosome 7, 8, 12, and 14 abnormalities by high-resolution tile-path array CGH

Chromosome-specific tile-path array CGH was performed in 16 primary cases and seven PEL cell lines. For chromosomes 7, 8, and 14, tile-path array CGH essentially confirmed the findings by 1 Mb array CGH and did not show any cryptic amplifications or deletions undetected by 1 Mb array CGH. Nevertheless, tile-path array CGH allowed further mapping of the MCR of amplification on chromosome 12.

Of the 23 cases investigated by tile-path array CGH, one each showed amplification at 12q13.2–15 and 12q21.2, and four cases displayed amplification at 12q23.3–24.11 by 1 Mb array CGH. Tile-path array CGH confirmed each of these findings by 1 Mb array CGH. For the amplifications at 12q13.2–15 and 12q21.2, tile-path array CGH did not show any cryptic amplification undetected by 1 Mb array CGH. Within the amplification at 12q13.2–15, there were a
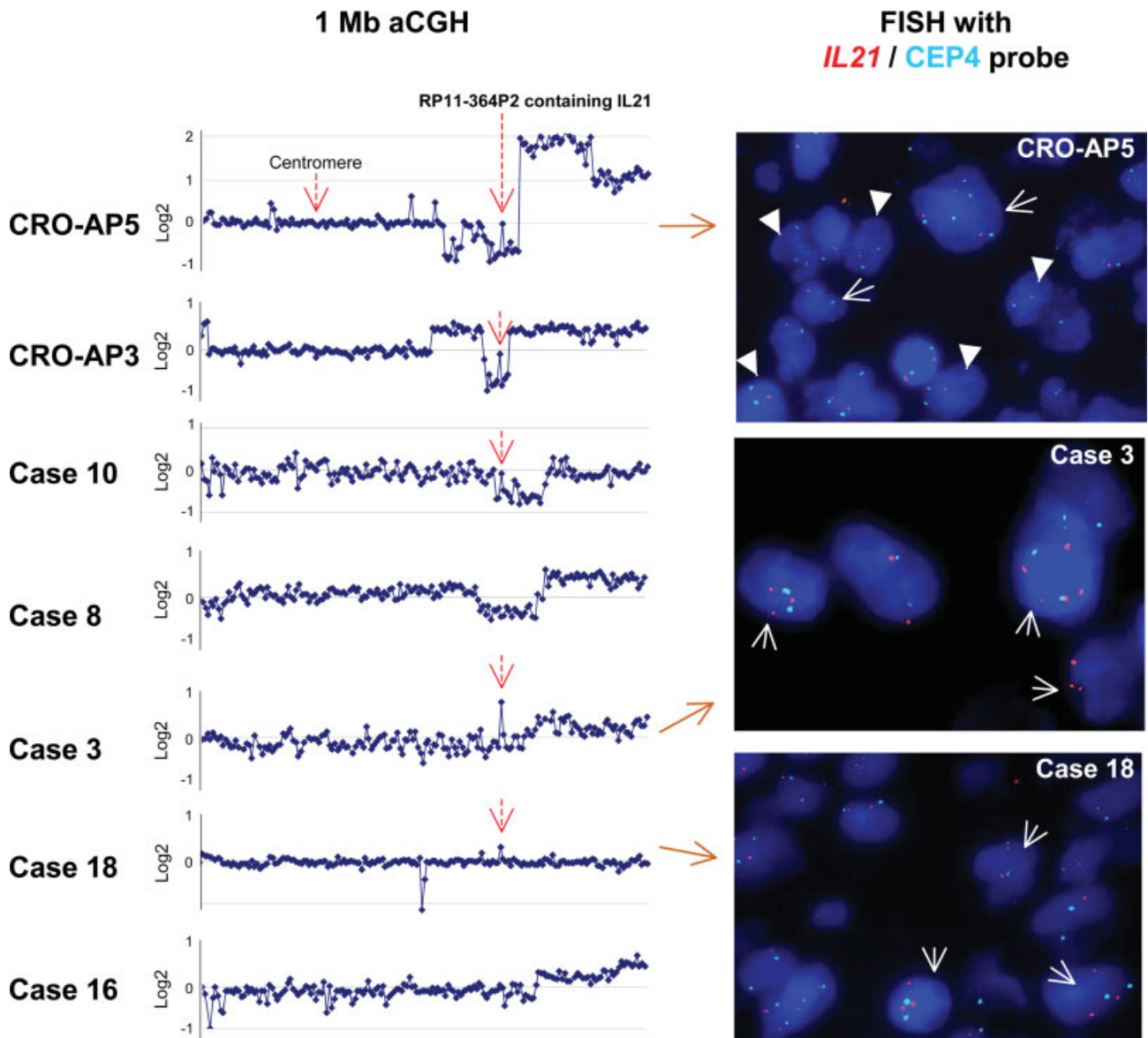
1 Mb aCGH

FISH with
IL21 / CEP4 probe

Figure 2. Examples of chromosome 4 abnormalities identified by 1 Mb array CGH and interphase FISH. PEL cell lines CRO-AP5 and CRO-AP3 and cases 10 and 8 show deletion at 4q26–28.2. The BAC clone RP11-364P2 containing *IL21* within the deletion was 'retained' in the first three cases. Interphase FISH in CRO-AP5 shows that the majority of tumour cells have one copy of the *IL21* locus (indicated by arrowheads), but a subpopulation of tumour cells gain at least one extra copy of the *IL21* locus (arrow). Gain of this BAC clone is also notable in cases 3 and 18 without the 4q26–28.2 deletion and interphase FISH confirms the gain of one to three extra copies of the *IL21* locus in a subset of tumour cells in these cases. Case 16 shows no copy number changes of RP11-364P2 by 1 Mb array CGH, but FISH shows the gain of four extra copies of the locus.

number of genes including *MDM2, IL22, IL23A, IL26, STAT2, STAT6*, and *CDK4*, potentially important for tumourigenesis. Within the amplification at 12q21.2, there were no obvious oncogenes.

For the amplification at 12q23.3–24.11, tile-path array CGH identified a cryptic amplification in two primary cases, which was not seen by 1 Mb array CGH (Figure 3). In one case (No 1), RP11-457O10, spanning a region of 181 kb at 12q24.11, was exclusively amplified to ∼13 copies, while in the other case (No 15) this BAC clone together with RP11-63B6 was amplified to ∼24 copies. Of the other four cases showing 12q23.3–24.11 amplification, tile-path array CGH showed that RP11-457O10 was almost invariably at the peak of the amplification.

Together, these findings indicated that RP11-457O10 represented the MCR of amplification at 12q24.11. There were only two genes within this MCR and they were selectin-P ligand (*SELPLG*) and coronin-1C (*CORO1C*) [31]. *SELPLG* encodes a protein critical for cell migration and chemotaxis, and was shown to be highly expressed in PEL by expression microarray studies [32,33]. *CORO1C* belongs to the coronin gene family, which regulates actin-dependent processes such as cell motility and vesicle trafficking, and its expression is critical for the motility and invasion of the malignant cells of diffuse glioblastomas [26,34]. In light of the above findings, our subsequent investigations focused on *SELPLG* and *CORO1C*.
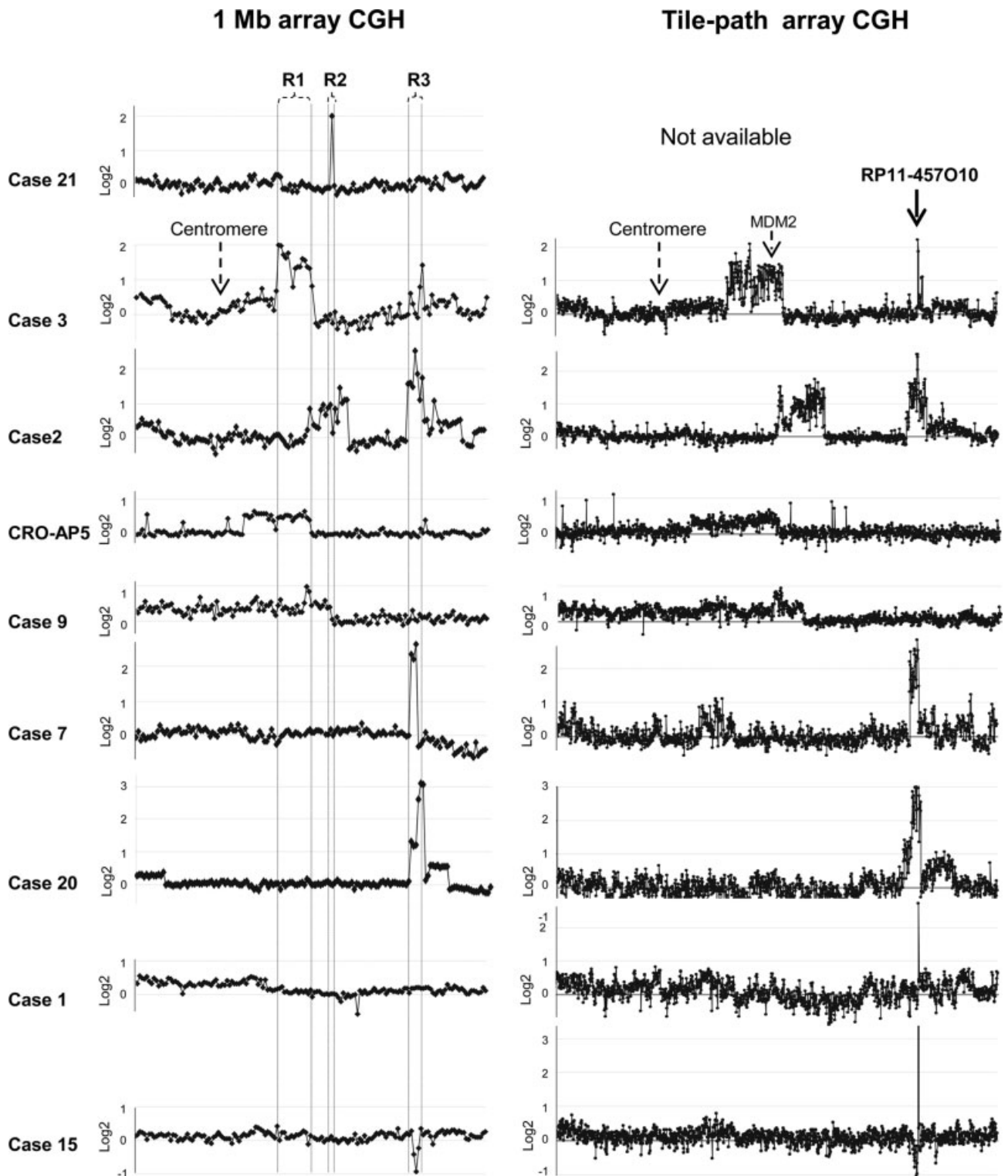
Figure 3. Chromosome 12 abnormalities identified by 1 Mb resolution and high-resolution tile-path array CGH. 1 Mb resolution array CGH shows three amplified regions: a 14.7 Mb region at 12q13.2–15 (R1); a 170 kb region at 12q21.2 (R2); and a 3.28 Mb region at 12q23.3–24.11 (R3). High-resolution tile-path array confirms the findings by 1 Mb array CGH in each case and reveals cryptic amplification at 12q24.11 in cases 1 and 15, which is undetected by 1 Mb array CGH. In case 1, RP11-457O10, spanning a region of 181 kb at 12q24.11, is exclusively amplified to approximately 13 copies, while in case 15, this BAC clone together with RP11-63B6 is amplified to approximately 24 copies. RP11-457O10 is also invariably at the peak of the amplification in other cases. There are two genes of particular interest, namely *SELPLG* and *CORO1C*, in the region of RP11-457O10.
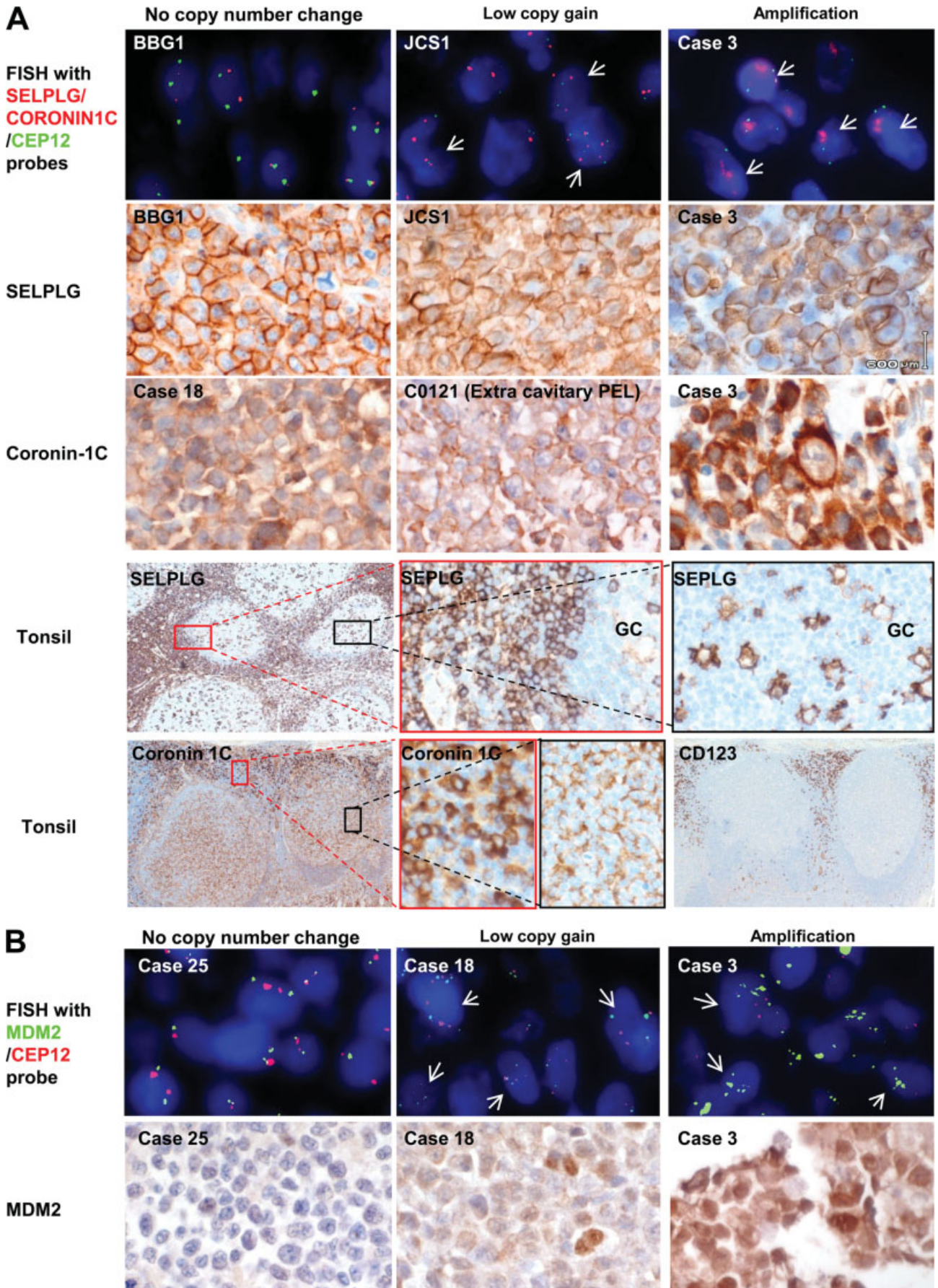
Figure 4.

Characterization of abnormalities by FISH, qPCR, and immunohistochemistry

Among several BAC clones tested, only RP11-266G20, which overlaps with RP11-457O10 but does not contain the *SELPLG* and *CORO1C* genes, gave specific and adequate FISH signals. Interphase FISH with the labelled RP11-266G20 and CEP12 was successfully performed on cell clots of 26 PELs including four showing amplification (three cases) or low-level gain (one case) of the *SELPLG/CORO1C* locus by array CGH (Figure 4). Interphase FISH confirmed the alterations identified by array CGH and in total identified *SELPLG/CORO1C* amplification in 6 PELs (23%), low-level copy number gain in six PELs (23%), and loss of one copy in one PEL (4%).

To further ascertain the above interphase FISH findings, we separately measured the copy number of *SELPLG* and *CORO1C* by qPCR in 35 cases of PEL including 13 that showed no change, seven that displayed low copy number gain, and six that showed *SELPLG/CORO1C* gene amplification by tile-path array CGH and/or interphase FISH, and nine further cases without array CGH or FISH data. There was an excellent correlation between the *SELPLG* and *CORO1C* qPCR results ($R = 0.875$, $p = 0.0001$) (Figure 5). qPCR confirmed each of the six cases showing *SELPLG/CORO1C* gene amplification by tile-path array CGH and/or interphase FISH. Based on the mean ± 3 SDs of the cases showing low copy number of gain as the threshold value for diagnosis of gene amplification, two cases (one from the group showing no change and the other from the group without array CGH or FISH data) showed ΔCT values above this threshold, compatible with those of cases showing the gene amplification (Figure 5). Thus, these two cases should be regarded as those with the gene amplification. Accordingly, eight of the 35 cases (23%) investigated showed evidence of *SELPLG* and *CORO1C* gene amplification.

To determine the impact of *SELPLG* gene dosage changes on its protein expression, we performed immunohistochemistry. Most of the PELs ($24/26 = 92\%$) showed uniform moderate to strong SELPLG staining in more than 70% of lymphoma cells (Figure 4), while the remaining cases, including the case showing hemizygous *SELPLG/CORO1C* deletion by FISH, were negative. Overall, there was no apparent difference in the staining intensity or percentage of positive cells among cases with various *SELPLG* gene dosages.

Similar to SELPLG, the majority of PELs ($15/21 = 71\%$) showed strong to moderate coronin-1C staining in more than 70% of lymphoma cells (Figure 4). There was no apparent difference in the staining intensity or percentage of positive cells among cases with various *CORO1C* gene dosages. Interestingly, reactive tonsils showed no apparent SELPLG and coronin-1C staining in B cells. However, SELPLG was highly expressed in germinal centre macrophages and interfollicular T-cells while coronin-1C was highly expressed in plasmacytoid dendritic cells and moderately in germinal centre macrophages and follicular dendritic cells (Figure 4).

Since immunohistochemistry is not a perfect quantitative method and is greatly affected by tissue processing and fixation conditions, we further investigated the correlation between the *SEPLG/CORO1C* gene dosage and their protein expression by qPCR and western blot (Figure 5D). Among the seven PEL cell lines investigated, BC3 showed both the highest *SELPLG* gene dosage and the highest protein expression. ISI1, BCP1, and BBG1 showed a moderate increase of the *SELPLG* gene dosage and a high level of protein expression. Nonetheless, HBL6 and BCBL1 showed no change of the *SELPLG* gene dosage, but displayed moderate protein expression. In contrast, BC3 showed the highest *CORO1C* gene dosage, but displayed only moderate protein expression, much less than that of BCP1, which showed a moderately increased gene dosage. ISI1 showed no change of the *CORO1C* gene dosage, but expressed a high level of the protein.

Interphase FISH with *MDM2/CEP12* probes was performed in 27 PELs including four showing copy number changes at this genomic locus (amplification in one case; low copy gain in three cases) by array CGH (Figure 3). Interphase FISH confirmed the array CGH-identified *MDM2* copy number changes in these cases and in total, identified *MDM2* amplification in two PELs (7%) and low levels of copy number gain in 15 PELs (56%).

MDM2 immunohistochemistry was performed in 25 cases including two and 13 cases showing *MDM2* amplification and low-level copy number gain, respectively. Five cases showed strong to moderate staining in more than 70% cells; four cases displayed weak staining in more than 70% cells; and three further cases showed weak staining in 30–70% cells. The remaining 13 cases were negative. There was no apparent correlation between *MDM2* gene dosage changes and the results of immunohistochemistry, although the

Figure 4. Investigation of *SELPLG/CORO1C, MDM2* abnormalities by interphase FISH and immunohistochemistry. (A) Upper panel: examples of interphase FISH showing PEL with no copy number change, low-level copy number gain (one to four extra copies), and amplification at the *SELPLG/CORO1C* locus. The probe for *SELPLG/CORO1C* is labelled with SpectrumOrange; the CEP12 probe is labelled with SpectrumGreen. Corresponding results of SELPLG and CORO1C immunohistochemistry are shown below. Lower panels: expression pattern of SELPLG and coronin-1C in a reactive tonsil. SELPLG is highly expressed in germinal centre macrophages and interfollicular T cells, while coronin-1C is highly expressed in a subset of interfollicular cells, consistent with the distribution of plasmacytoid dendritic cells, and moderately expressed in germinal centre macrophages and follicular dendritic cells. CD123 staining highlights plasmacytoid dendritic cells. GC = germinal centre. (B) Examples of interphase FISH showing PEL with no copy number change, low-level copy number gain (one to four extra copies), and amplification at the *MDM2* locus. *MDM2* is labelled with SpectrumGreen, while CEP12 is labelled with SpectrumOrange. Corresponding results of MDM2 immunohistochemistry are shown below.
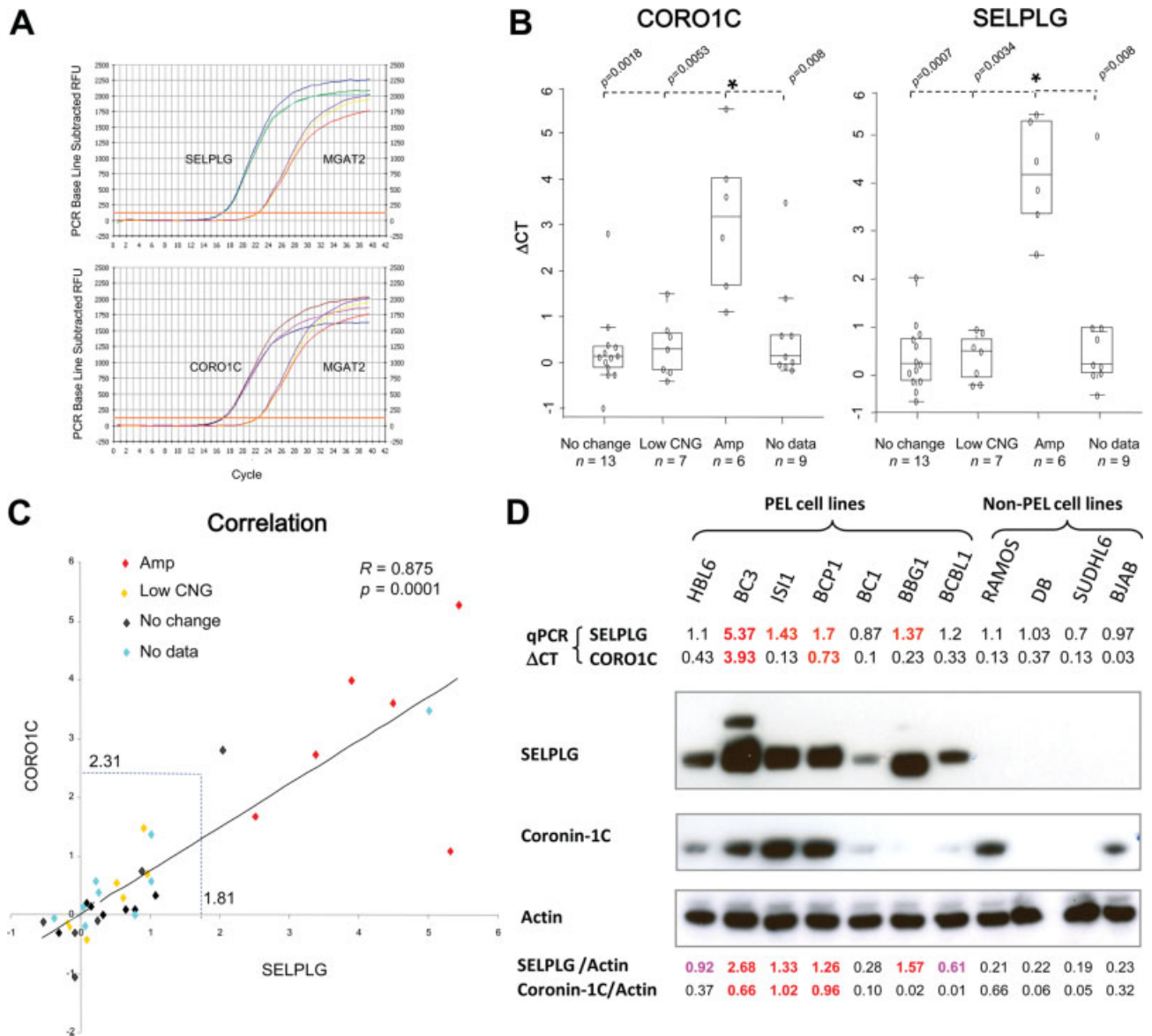
Figure 5. Investigation of *SELPLG* and *CORO1C* amplification by qPCR and western blot analysis. (A) Example of qPCR for *SELPLG* and *CORO1C* with the *MAGT2* gene (α-1,6-mannosyl-glycoprotein 2-beta-*N*-acetylglucosaminyltransferase) being used as a reference control. *MAGT2* resides at 14q21.3, which showed no copy number changes by 1 Mb and tile-path array CGH. (B) qPCR confirms all six cases showing *SELPLG/CORO1C* gene amplification by tile-path array CGH and/or interphase FISH. In addition, qPCR identifies two further cases (one from the group showing no change and one from the group without array CGH or FISH data) which show ΔCT values above the threshold (mean ±3 SDs) (based on the cases showing low copy number of gain) for diagnosis of *SELPLG* (1.81) and *CORO1C* (2.31) gene amplification. (C) Correlation between the *SELPLG* and *CORO1C* qPCR results. (D) Correlation between *SELPLG/CORO1C* gene dosages and their protein expression. BC3 shows the highest *SELPLG* gene dosage by qPCR and the greatest protein expression by western blot, followed by ISI1, BCP1, and BBG1, which display a moderate increase in gene dosage and also a high level of protein expression. Nonetheless, HBL6 and BCBL1 show no evidence of increased *SELPLG* gene dosage, but display moderate protein expression. BC3 also shows the highest *CORO1C* gene dosage, but only moderate protein expression. BCP1 displays both a moderately increased *CORO1C* gene dosage and moderately increased protein expression. However, ISI1 shows no increase in gene dosage, but expresses a high level of the protein. Low CNG = low copy number gain; Amp = amplification.

two cases with *MDM2* amplification showed uniform MDM2 staining, of strong intensity in one case and weak intensity in the other.

Interphase FISH with *IL21*/CEP4 probes was performed in 23 PELs including two (CRO-AP3 and CRO-AP5) showing 'retention' of the *IL21* locus within the 4q26–28.2 deletion, one case (No 3) with an apparent gain, and another case with a moderate gain of this locus (Figure 2). Of the two cases with 4q26–28.2 deletion, one case showed two copies,

and hence 'retention', of the *IL21* locus by interphase FISH, while the other case showed one copy in the majority of cells but gain of one to three extra copies in a subset of the tumour cells. In the two cases with variable gain of the *IL21* locus but without 4q26–28.2 deletion, gain of one to three extra copies of the *IL21* locus was seen in a subset of the tumour cells. In total, interphase FISH clearly demonstrated gain (one to four extra copies) of the *IL21* locus in the majority of tumour cells in 6/23 (26%) cases. Gain of one

to three extra copies of the *IL21* locus was also seen in a subset (8–12%) of the tumour cells, above the threshold value, in a further three cases.

Discussion

Our present study revealed numerous genomic gains/amplifications and losses in the vast majority of PELs. Despite such extensive alterations, several genomic regions frequently affected in other aggressive B-cell lymphomas are largely spared in PEL and several strands of evidence raise the possibility of potential cooperation between cellular genetic events and KSHV-associated oncogenic products in the development of PEL. For example, the *TP53* (17p13) and *RB* (13q14) loci were not deleted and the *MYC* locus (8q24), although frequently involved as part of 8q gain, was rarely amplified. These findings are in keeping with previous observations of a lack of *TP53* mutation and *MYC* amplification/gene rearrangement in PEL [5,19,35,36]. Nonetheless, the products of these cellular genes are deregulated at the protein level by KSHV LANA-1 and their deregulation is critical for the development of KSHV-associated malignancies [37–39]. LANA-1 directly interacts with p53 and MDM2, inactivating the transcriptional activity of p53 and its ability to induce apoptosis, thus promoting cell survival and chromosomal instability [37,38,40]. Reactivation of the p53 pathway by MDM2 inhibitor induces massive apoptosis of PEL cells [38]. Moreover, LANA-1 also binds to and inactivates Rb, thereby releasing the transcription factor E2F and promoting cell cycle progression [39]. Finally, LANA-1 binds to and inhibits glycogen synthase kinase (GSK)-3β, preventing GSK-3β-medicated c-Myc phosphorylation and consequently increasing c-Myc stability [41]. The deregulation of p53, Rb, and Myc at the protein level by LANA-1 potentially explains the absence of their genetic abnormalities in PEL.

The most frequent copy number alterations were gains/amplifications at 1q21–41(47%), 4q28.3–35 (29%), 7q (58%), 8q (63%), 11 (32%), 12 (61%), 17q (29%), 19p (34%), and 20q (34%), and deletion of 4q (32%), 11q25, (29%) and 14q32 (63%). Among the gains/amplifications, those found on chromosome 12 were the most remarkable. By high-resolution tile-path array CGH, we identified a single BAC clone (RP11-457O10), spanning a 181 kb region at 12q24.11, as the MCR of the amplification. There were two genes, namely *SELPLG* and *CORO1C*, in this MCR. Subsequent interphase FISH and qPCR demonstrated amplification and low levels of gain of the *SELPLG/CORO1C* locus in 23% of PELs. Irrespective of the gene copy number, immunohistochemistry demonstrated strong homogeneous SELPLG and coronin-1C staining in the majority of PELs. Since immunohistochemistry is not a perfect quantitative method and also depends critically on tissue processing

and fixation conditions, it may not be sensitive enough to detect differences in protein expression between cases with various gene dosages. By qPCR and western blot, we demonstrated a general correlation between the *SELPLG* gene dosage and its protein expression, but not between the *CORO1C* gene dosage and its protein expression. Some PEL cell lines showed no change in the *SELPLG* and *CORO1C* gene dosages but displayed high levels of their protein expression. This finding strongly indicates that there are other mechanisms which up-regulate the expression of these proteins [42]. Interestingly, SELPLG was not expressed in other non-Hodgkin lymphomas [32,33] or in cell lines derived from DLBCL (DB and SUDHL6) and Burkitt lymphoma (RAMOS and BJAB), although it was expressed in KSHV-negative AIDS-associated DLBCL [43]. In addition, there is no apparent expression of these proteins in B cells of reactive tonsils. Together, these findings indicate aberrant SELPLG and coronin-1C expression in PEL.

SELPLG encodes a membrane-associated glycoprotein that binds to not only P-selectin, but also E- and L-selectin. Among normal haematopoietic cells, SELPLG is highly expressed in myeloid, dendritic, and T cells [44]. SELPLG is involved in the tethering and rolling of leukocytes on activated endothelial cells, and is thus important for the recruitment of leukocytes to sites of inflammation. The role of SELPLG expression in lymphoma pathogenesis remains unknown. Nonetheless, in a murine lymphoma metastasis model, SELPLG expression was critical for lymphoma cell colonization and tumour formation in the liver and spleen [45]. In addition, SELPLG also functions as a signal transduction receptor. For example, engagement of SELPLG triggers intracellular signal events leading to the redistribution of F-actin-based cytoskeleton and up-regulation of CSF-1 transcription [46,47].

CORO1C belongs to the coronin gene family, which regulates actin-dependent processes such as cell motility and vesicle trafficking [34]. In a number of solid tumours, coronin-1C expression is associated with invasion and metastasis [26,34]. The role of coronin-1C in normal and malignant lymphoid cells is currently unknown. Nonetheless, it has been shown that coronin-1A regulates F-actin formation and also plays a role in lymphocyte homeostasis and survival [48]. By comparative analysis of the gene and protein expression profiles of the effusion and solid lymphomas derived from the same PEL cell line in a mouse model, coronin-1A was identified to be highly expressed in the solid lymphoma [49]. In view of these findings, both SELPLG and CORO1C expression may play an important role in PEL pathogenesis, mostly likely by promoting the lymphoma cells to colonize and grow in body cavities and extranodal sites.

The amplification at 12q15–21.2 contains a number of genes including *MDM2, STAT2, STAT6*, and *CDK4*, potentially important for PEL pathogenesis. However, only one PEL showed the amplification and tile-path array CGH did not reveal any cryptic amplification

within this genomic region in other cases. Additional investigation by interphase FISH and immunohisto-chemistry showed *MDM2* amplification in a small proportion of PELs (7%) and strong to moderate MDM2 staining in a higher proportion of cases (20%). These findings suggest a role for MDM2 overexpression in PEL pathogenesis.

Among the five cases with 4q26–28.2 deletion, the BAC clone RP11-364P2 within the deletion was 'retained' in four (either truly retained or appeared to be 'retained' due to the presence of extra copies in a subset of tumour cells) and this clone was also targeted for a moderate gain in 26% of cases. Several genes in this genomic region, including *GPCR103, CYCLIN-A2, IL21*, and basic *FGF2*, are potentially relevant in lymphoma pathogenesis. Among them, *IL21* and *FGF2* are particularly interesting. IL21 acts as a powerful growth factor for B cells and also induces the production of IL-10 [50], which is a potent autocrine growth factor for PEL cells [51]. FGF is a strong pro-angiogenic cytokine, well known for its role in tumour growth and angiogenesis in a wide spectrum of human cancers including leukaemia and lymphoma [52]. Both IL21 and FGF can be secreted and can potentially exert their oncogenic effect through autocrine and paracrine stimulations.

In summary, we have shown extensive genomic gains/amplifications and losses in PEL and have identified *SELPLG* and *CORO1C* as the targets of amplification at 12q24.11. It remains to be investigated whether these cellular genetic changes are also common to other KSHV-associated-LPDs and how these genetic alterations cooperate with the KSHV-associated oncogenic products in lymphomagenesis.

Acknowledgment

Author contribution statement

SL collected and analysed the data and drafted major parts of the manuscript. EB provided the majority of PELs used for the study and contributed to the study design. HY, EC, NJ, RAH, HL, and YH collected and analysed the data. CMB, JS, PC, EC, AC, and PGI provided cases. CSC provided the coronin-1C antibody. MQD designed, analysed the data, and wrote the manuscript.

References

1. Du MQ, Bacon CM, Isaacson PG. Kaposi sarcoma-associated herpesvirus/human herpesvirus 8 and lymphoproliferative disorders. *J Clin Pathol* 2007; **60**: 1350–1357.

2. Cesarman E, Mesri EA. Kaposi sarcoma-associated herpesvirus and other viruses in human lymphomagenesis. *Curr Top Microbiol Immunol* 2007; **312**: 263–287.

3. Boulanger E, Gerard L, Gabarre J, *et al*. Prognostic factors and outcome of human herpesvirus 8-associated primary effusion lymphoma in patients with AIDS. *J Clin Oncol* 2005; **23**: 4372–4380.

4. Chadburn A, Hyjek E, Mathew S, *et al*. KSHV-positive solid lymphomas represent an extra-cavitary variant of primary effusion lymphoma. *Am J Surg Pathol* 2004; **28**: 1401–1416.

5. Nador RG, Cesarman E, Chadburn A, *et al*. Primary effusion lymphoma: a distinct clinicopathologic entity associated with the Kaposi's sarcoma-associated herpes virus. *Blood* 1996; **88**: 645–656.

6. Verma SC, Lan K, Robertson E. Structure and function of latency-associated nuclear antigen. *Curr Top Microbiol Immunol* 2007; **312**: 101–136.

7. Dupin N, Fisher C, Kellam P, *et al*. Distribution of human herpesvirus-8 latently infected cells in Kaposi's sarcoma, multicentric Castleman's disease, and primary effusion lymphoma. *Proc Natl Acad Sci U S A* 1999; **96**: 4546–4551.

8. Carbone A, Gloghini A, Bontempo D, *et al*. Proliferation in HHV-8-positive primary effusion lymphomas is associated with expression of HHV-8 cyclin but independent of p27(kip1). *Am J Pathol* 2000; **156**: 1209–1215.

9. Teruya-Feldstein J, Zauber P, Setsuda JE, *et al*. Expression of human herpesvirus-8 oncogene and cytokine homologues in an HIV-seronegative patient with multicentric Castleman's disease and primary effusion lymphoma. *Lab Invest* 1998; **78**: 1637–1642.

10. Luppi M, Barozzi P, Maiorana A, *et al*. Expression of cell-homologous genes of human herpesvirus-8 in human immunodeficiency virus-negative lymphoproliferative diseases. *Blood* 1999; **94**: 2931–2933.

11. Low W, Harries M, Ye H, *et al*. Internal ribosome entry site regulates translation of Kaposi's sarcoma-associated herpesvirus FLICE inhibitory protein. *J Virol* 2001; **75**: 2938–2945.

12. Lubyova B, Kellum MJ, Frisancho AJ, *et al*. Kaposi's sarcoma-associated herpesvirus-encoded vIRF-3 stimulates the transcriptional activity of cellular IRF-3 and IRF-7. *J Biol Chem* 2004; **279**: 7643–7654.

13. Horenstein MG, Nador RG, Chadburn A, *et al*. Epstein–Barr virus latent gene expression in primary effusion lymphomas containing Kaposi's sarcoma-associated herpesvirus/human herpesvirus-8. *Blood* 1997; **90**: 1186–1191.

14. Szekely L, Chen F, Teramoto N, *et al*. Restricted expression of Epstein–Barr virus (EBV)-encoded, growth transformation-associated antigens in an EBV- and human herpesvirus type 8-carrying body cavity lymphoma line. *J Gen Virol* 1998; **79**: 1445–1452.

15. Fassone L, Bhatia K, Gutierrez M, *et al*. Molecular profile of Epstein–Barr virus infection in HHV-8-positive primary effusion lymphoma. *Leukemia* 2000; **14**: 271–277.

16. Katano H, Hoshino Y, Morishita Y, *et al*. Establishing and characterizing a CD30-positive cell line harboring HHV-8 from a primary effusion lymphoma. *J Med Virol* 1999; **58**: 394–401.

17. Gaidano G, Capello D, Fassone L, *et al*. Molecular characterization of HHV-8 positive primary effusion lymphoma reveals pathogenetic and histogenetic features of the disease. *J Clin Virol* 2000; **16**: 215–224.

18. Wilson KS, McKenna RW, Kroft SH, *et al*. Primary effusion lymphomas exhibit complex and recurrent cytogenetic abnormalities. *Br J Haematol* 2002; **116**: 113–121.

19. Carbone A, Cilia AM, Gloghini A, *et al*. Establishment and characterization of EBV-positive and EBV-negative primary effusion lymphoma cell lines harbouring human herpesvirus type-8. *Br J Haematol* 1998; **102**: 1081–1089.

20. Boulanger E, Duprez R, Delabesse E, *et al*. Mono/oligoclonal pattern of Kaposi sarcoma-associated herpesvirus (KSHV/HHV-8) episomes in primary effusion lymphoma cells. *Int J Cancer* 2005; **115**: 511–518.

21. Said J, Cesarman E. Primary effusion lymphoma. In *WHO Classification of Tumours of Haematopoietic and Lymphoid Tissues*, Swerdlow SH, Campo E, Harris NL, *et al*. (eds). International Agency for Research on Cancer: Lyon, 2008; 260–261.

22. Johnson NA, Hamoudi RA, Ichimura K, *et al*. Application of array CGH on archival formalin-fixed paraffin-embedded tissues including small numbers of microdissected cells. *Lab Invest* 2006; **86**: 968–978.

23. Chanudet E, Ye H, Ferry J, *et al*. A20 deletion is associated with copy number gain at the TNFA/B/C locus and occurs preferentially in translocation-negative MALT lymphoma of the ocular adnexa and salivary glands. *J Pathol* 2009; **217**: 420–430.

24. Kahl C, Gesk S, Harder L, *et al*. Detection of translocations involving the HOX11/TCL3-locus in 10q24 by interphase fluorescence *in situ* hybridization. *Cancer Genet Cytogenet* 2001; **129**: 80–84.

25. Ye H, Gong L, Liu H, *et al*. MALT lymphoma with t(14;18)(q32;q21)/IGH-MALT1 is characterized by strong cytoplasmic MALT1 and BCL10 expression. *J Pathol* 2005; **205**: 293–301.

26. Thal D, Xavier CP, Rosentreter A, *et al*. Expression of coronin-3 (coronin-1C) in diffuse gliomas is related to malignancy. *J Pathol* 2008; **214**: 415–424.

27. Spoerl Z, Stumpf M, Noegel AA, *et al*. Oligomerization, F-actin interaction, and membrane association of the ubiquitous mammalian coronin 3 are mediated by its carboxyl terminus. *J Biol Chem* 2002; **277**: 48858–48867.

28. Morita R, Fujita T, Uchiyama T, *et al*. Human plasmacytoid dendritic cells express an atrial natriuretic peptide receptor, guanylyl cyclase-A. *Microbiol Immunol* 2009; **53**: 403–411.

29. Shaikh TH, Gai X, Perin JC, *et al*. High-resolution mapping and analysis of copy number variations in the human genome: a data resource for clinical and research applications. *Genome Res* 2009; **19**: 1682–1690.

30. Capello D, Gaidano G, Gallicchio M, *et al*. The tyrosine kinase receptor met and its ligand HGF are co-expressed and functionally active in HHV-8 positive primary effusion lymphoma. *Leukemia* 2000; **14**: 285–291.

31. Morgan RO, Fernandez MP. Molecular phylogeny and evolution of the coronin gene family. *Subcell Biochem* 2008; **48**: 41–55.

32. Klein U, Gloghini A, Gaidano G, *et al*. Gene expression profile analysis of AIDS-related primary effusion lymphoma (PEL) suggests a plasmablastic derivation and identifies PEL-specific transcripts. *Blood* 2003; **101**: 4115–4121.

33. Arguello M, Paz S, Hernandez E, *et al*. Leukotriene A4 hydrolase expression in PEL cells is regulated at the transcriptional level and leads to increased leukotriene B4 production. *J Immunol* 2006; **176**: 7051–7061.

34. Roadcap DW, Clemen CS, Bear JE. The role of mammalian coronins in development and disease. *Subcell Biochem* 2008; **48**: 124–135.

35. Katano H, Sato Y, Sata T. Expression of p53 and human herpesvirus-8 (HHV-8)-encoded latency-associated nuclear antigen with inhibition of apoptosis in HHV-8-associated malignancies. *Cancer* 2001; **92**: 3076–3084.

36. Boulanger E, Marchio A, Hong SS, *et al*. Mutational analysis of TP53, PTEN, PIK3CA and CTNNB1/beta-catenin genes in human herpesvirus 8-associated primary effusion lymphoma. *Haematologica* 2009; **94**: 1170–1174.

37. Si H, Robertson ES. Kaposi's sarcoma-associated herpesvirus-encoded latency-associated nuclear antigen induces chromosomal instability through inhibition of p53 function. *J Virol* 2006; **80**: 697–709.

38. Sarek G, Kurki S, Enback J, *et al*. Reactivation of the p53 pathway as a treatment modality for KSHV-induced lymphomas. *J Clin Invest* 2007; **117**: 1019–1028.

39. Radkov SA, Kellam P, Boshoff C. The latent nuclear antigen of Kaposi sarcoma-associated herpesvirus targets the retinoblastoma–E2F pathway and with the oncogene Hras transforms primary rat cells. *Nature Med* 2000; **6**: 1121–1127.

40. Friborg J Jr, Kong W, Hottiger MO, *et al*. p53 inhibition by the LANA protein of KSHV protects against cell death. *Nature* 1999; **402**: 889–894.

41. Bubman D, Guasparri I, Cesarman E. Deregulation of c-Myc in primary effusion lymphoma by Kaposi's sarcoma herpesvirus latency-associated nuclear antigen. *Oncogene* 2007; **26**: 4979–4986.

42. Roadcap DW, Clemen CS, Bear JE. The role of mammalian coronins in development and disease. *Subcell Biochem* 2008; **48**: 124–135.

43. Carbone A, Gloghini A, Vaccher E, *et al*. Kaposi's sarcoma-associated herpesvirus/human herpesvirus type 8-positive solid lymphomas: a tissue-based variant of primary effusion lymphoma. *J Mol Diagn* 2005; **7**: 17–27.

44. Laszik Z, Jansen PJ, Cummings RD, *et al*. P-selectin glycoprotein ligand-1 is broadly expressed in cells of myeloid, lymphoid, and dendritic lineage and in some nonhematopoietic cells. *Blood* 1996; **88**: 3010–3021.

45. Raes G, Ghassabeh GH, Brys L, *et al*. The metastatic T-cell hybridoma antigen/P-selectin glycoprotein ligand 1 is required for hematogenous metastasis of lymphomas. *Int J Cancer* 2007; **121**: 2646–2652.

46. Ba XQ, Chen CX, Xu T, *et al*. Engagement of PSGL-1 upregulates CSF-1 transcription via a mechanism that may involve Syk. *Cell Immunol* 2005; **237**: 1–6.

47. Ba X, Chen C, Gao Y, *et al*. Signaling function of PSGL-1 in neutrophil: tyrosine-phosphorylation-dependent and c-Abl-involved alteration in the F-actin-based cytoskeleton. *J Cell Biochem* 2005; **94**: 365–373.

48. Foger N, Rangell L, Danilenko DM, *et al*. Requirement for coronin 1 in T lymphocyte trafficking and cellular homeostasis. *Science* 2006; **313**: 839–842.

49. Yanagisawa Y, Sato Y, Asahi-Ozaki Y, *et al*. Effusion and solid lymphomas have distinctive gene and protein expression profiles in an animal model of primary effusion lymphoma. *J Pathol* 2006; **209**: 464–473.

50. Good KL, Bryant VL, Tangye SG. Kinetics of human B cell behavior and amplification of proliferative responses following stimulation with IL-21. *J Immunol* 2006; **177**: 5236–5247.

51. Jones KD, Aoki Y, Chang Y, *et al*. Involvement of interleukin-10 (IL-10) and viral IL-6 in the spontaneous growth of Kaposi's sarcoma herpesvirus-associated infected primary effusion lymphoma cells. *Blood* 1999; **94**: 2871–2879.

52. Ribatti D, Vacca A, Rusnati M, *et al*. The discovery of basic fibroblast growth factor/fibroblast growth factor-2 and its role in haematological malignancies. *Cytokine Growth Factor Rev* 2007; **18**: 327–334.

SUPPORTING INFORMATION ON THE INTERNET

The following supporting information may be found in the online version of this article.

Supplementary methods.

Figure S1. Genomic profiles of PEL by 1 Mb resolution array CGH.

Figure S2. Chromosome 7 abnormalities identified by 1 Mb resolution and high-resolution tile-path array CGH.

Figure S3. Chromosome 8 abnormalities identified by 1 Mb resolution and high-resolution tile-path array CGH.

Figure S4. Chromosome 14q deletion identified by 1 Mb resolution and high resolution tile-path array CGH.

1 Mb resolution array CGH data.

Tile-path array CGH data.